GEOPHYSICAL RESEARCH LETTERS, VOL. 39, L22804, doi:10.1029/2012GL053388, 2012

Transport of black carbon to polar regions: Sensitivity and forcing by black carbon

Cheng Zhou,[1] Joyce E. Penner,[1] Mark G. Flanner,[1] Marion M. Bisiaux,[2] Ross Edwards,[3] and Joseph R. McConnell[2]

Received 31 July 2012; revised 24 October 2012; accepted 24 October 2012; published 28 November 2012.

[1] The transport of black carbon (BC) to polar regions is studied using the University of Michigan IMPACT aerosol model driven by two sets of meteorological fields from the NCAR CAM5 and GFDL AM3 models. The sensitivity of the transport of BC to wet deposition processes is tested by varying the wet deposition in large-scale precipitation. BC concentrations and deposition in polar regions are shown to be sensitive to both the meteorological fields and the wet deposition treatment. Using the default wet deposition, both IMPACT-CAM5 and IMPACT-AM3 simulate an appropriate amount of BC deposition in polar regions as compared to ice core observations. Although the seasonal cycle of BC surface air concentrations is reasonable, the concentrations are about 1∼2 orders of magnitude smaller than observations. With reduced wet deposition efficiency, the total deposition of BC increases by a factor of ∼2 to ∼3 due to more transport to the poles. The near surface BC concentrations increase even more (by a factor of ∼3 to ∼10) but are still largely underestimated especially in the north polar region. The radiative forcing from the BC deposited on snow and sea ice is also sensitive to the wet deposition treatment and the different meteorological fields. The global (Arctic) annual mean forcing is about +0.020 W m^{-2} (+0.11 W m^{-2}) for IMPACT-CAM5 and +0.022 W m^{-2} (+0.13W m^{-2}) for IMPACT-AM3. **Citation:** Zhou, C., J. E. Penner, M. G. Flanner, M. M. Bisiaux, R. Edwards, and J. R. McConnell (2012), Transport of black carbon to polar regions: Sensitivity and forcing by black carbon, *Geophys. Res. Lett.*, *39*, L22804, doi:10.1029/2012GL053388.

1. Introduction

[2] Black carbon (BC) deposited to snow and sea-ice can reduce surface reflectance due to multiple scattering in the snowpack and the much larger absorption coefficients of BC than ice [e.g., *Warren and Wiscombe*, 1980]. This is of interest as the BC snow radiative effect can alter snow melt timing and spatial coverage. Estimates of the global average radiative forcing from BC due to altered surface albedos range from 0.01 to 0.16 W m^{-2} [*Hansen and Nazarenko*, 2004; *Hansen et al.*, 2007; *Flanner et al.*, 2007, 2009; *Koch et al.*, 2009a, 2009b; *Bauer and Menon*, 2012]. The uncertainty is partially related to uncertainty in the amount of BC transported to high latitudes. Factors that affect this transport include the treatment of BC aging, deposition (dry/wet), tracer advection, and the spatial and temporal variability of emission rates [*Koch et al.*, 2009a, 2009b; *Huang et al.*, 2010; *Liu et al.*, 2011].

[3] Here, we use the University of Michigan IMPACT aerosol model to test the sensitivity of the transport of BC as well as the resulting BC snow forcing to the meteorological fields and aerosol wet deposition treatment. The meteorological fields from the NCAR CAM5 model and the GFDL AM3 model are used to drive the IMPACT model with different wet deposition treatments. BC concentrations and deposition in polar regions are compared to observations at various sites. We also use the offline CESM CLM and CICE models to calculate the global radiative forcing caused by BC deposited to snow and sea-ice. Section 2 describes the model set-up. Section 3 presents the results followed by the conclusions and a discussion in Section 4.

2. Model Set-up

[4] The 3-mode offline version of the IMPACT aerosol model is used in this study [*Liu et al.*, 2005; *Wang et al.*, 2009]. It predicts the global distributions of sulfate, black carbon, organic matter, dust and sea salt using meteorological input from the NCAR Community Atmosphere Model (version 5) (CAM5, MAM3 aerosol module) and the GFDL AM3 model. Both CAM5 and AM3 use climatological sea surface temperature and anthropogenic aerosol emissions for year 2000 from CIMP5. Initial conditions are both from their developmental integrations. Readers are referred to *Liu et al.* [2012] and *Donner et al.* [2011] for more details of the model description, aerosol emissions and simulation biases. Comparisons of these two sets of meteorological fields, the performance of IMPACT when driven by them and emissions of aerosol species and their precursors are detailed in *Zhou et al.* [2012]. The total emission of BC is 10.51 Tg/year with 5.80 Tg/year from fossil/bio-fuel burning and 4.71 Tg/year from open biomass burning (updated from *Ito and Penner* [2005]) [*Wang et al.*, 2009].

[5] The wet scavenging scheme in IMPACT follows the Harvard wet scavenging model [*Giorgi and Chameides*, 1986; *Balkanski et al.*, 1993; *Mari et al.*, 2000; *Liu et al.*, 2001]. There are two types of wet scavenging: (1) scavenging in wet convective updrafts, and (2) first-order rainout and washout by large scale precipitation. From the middle to high latitudes, the wet deposition of BC is dominated by the

[1]Department of Atmospheric, Oceanic, and Space Sciences, University of Michigan, Ann Arbor, Michigan, USA.
[2]Division of Hydrologic Sciences, Desert Research Institute, Reno, Nevada, USA.
[3]Imaging and Applied Physics, Curtin University, Perth, Western Australia, Australia.

Corresponding author: C. Zhou, Department of Atmospheric, Oceanic, and Space Sciences, University of Michigan, Space Research Building, 2455 Hayward St., Ann Arbor, MI 48109-2143, USA. (zhouc@umich.edu)

0094-8276/12/2012GL053388

second type. To test the sensitivity of the transport of BC to wet deposition processes, we used two different values of the assumed condensed water content (liquid + ice) in large-scale precipitating clouds, 0.5 $cm^3\ m^{-3}$ and 1.5 $cm^3\ m^{-3}$ [see also *Liu et al.*, 2001], which controls the fraction of each gridbox experiencing precipitation, and thereby determines the magnitude of the latter type of wet scavenging. The larger value leads to a smaller area of the gridbox experiencing precipitation and thus less wet deposition of aerosols.

[6] Four basic 2-year simulations (C1, C2, A1, and A2) plus one sensitivity test case ($C2_{less}$) are performed. The two baseline cases, C1 and A1, use the meteorological fields from CAM5 and AM3 respectively, and the default condensed water content in precipitating clouds, 0.5 $cm^3\ m^{-3}$. C2 and A2 use the same meteorological fields as C1/A1 but with a larger assumed condensed water content, 1.5 $cm^3\ m^{-3}$. To reconcile the inconsistency between the BC surface air concentrations and ground deposition rates, we ran one additional case, $C2_{less}$, which is the same as C2 except with a reduced BC wet scavenge efficiency in ice clouds and an increased ice cloud fraction in mixed phase clouds. A thorough description of the dry and wet deposition treatments is available in the auxiliary material.[1]

[7] We used offline models for land and sea-ice to compute the BC radiative forcing in snow and sea-ice from the monthly dry/wet BC deposition fields calculated in the above four basic simulations. The offline models used prescribed reanalysis atmospheric states (from a combination of NCEP, GISS, and GCGCS). The land simulations applied the NCAR Community Land Model 4 (CLM) [*Lawrence et al.*, 2011], using bias-corrected atmospheric forcing data from *Qian et al.* [2006], run at 1.9 × 2.5 degree resolution. The sea-ice simulations applied the Community Ice CodE 4 (CICE). All runs were conducted using prescribed meteorology from 1994–2000, with 2 years of spin-up and 1996–2000 data averaged for the forcing calculation. Dust deposition fields were from a present-day climatology included with the NCAR Community Earth System Model 1. Monthly-resolved (annually-repeating) BC and dust deposition fields were linearly-interpolated to the model time step. The land snow and sea-ice treatments of aerosol processes and radiative transfer were described previously in *Flanner et al.* [2007], *Lawrence et al.* [2011] and *Holland et al.* [2012].

3. Results

[8] The global budgets, distributions, and atmospheric radiative forcing for all aerosol types are described in *Zhou et al.* [2012]. The main conclusion for BC is summarized here. Globally, case A1 simulates a higher BC burden (0.13 Tg vs. 0.11 Tg) and a longer BC lifetime (4.36 days vs. 3.64 days) than case C1. The larger BC burden of A1 is mainly in tropical regions where AM3 has a smaller convective mass flux than CAM5 and thus less wet scavenging in convective clouds. However, case A1 transports less BC to the Arctic than does case C1 due to two major factors. First, AM3 has more large-scale precipitation than CAM5 (1.11 mm/day vs. 0.87 mm/day) with most of the difference occurring in regions between 60°S and 60°N. Second, the in-cloud liquid water content and low cloud fraction from AM3 are larger than those from CAM5 in northern high latitudes. Therefore, there is more sulfate produced in aqueous phase reactions in A1. This leads to more sulfate coated on BC in A1 and thus increases its wet scavenging efficiency (see auxiliary material). In the runs with reduced wet deposition by large-scale precipitation, the global burden of BC increases: by 31% from A1 to A2 and by 18% from C1 to C2. The higher increase from A1 to A2 is due to greater large-scale precipitation in AM3 that makes A1/A2 more sensitive to this change.

[9] Figures 1a–1d show time-height plots of monthly averaged BC concentrations north of 80°N from cases C1, A1, C2 and A2. The four cases share some common characteristics. First, a distinct annual cycle with maximum BC concentrations appearing in late winter/early spring and minimum BC concentrations in late summer is present in all four cases, as also seen in observations (e.g., Figure 2). Second, there is a BC maximum near the surface in winter as well as a BC maximum in the upper troposphere in spring. This is related to the meridional BC mass flux vertical profiles in different seasons caused by the equatorward expansion of the polar dome in winter and its retreat starting in spring. With reduced wet deposition, C2 and A2 have higher BC concentrations than C1 and A1. This increase can be seen in the BC concentration ratios of C2 to C1 and A2 to A1, which are shown in Figures 1e and 1f. BC concentrations near the surface are more sensitive to this change since most precipitation in the Arctic forms in the lower troposphere. The ratio is also more sensitive during the summer and fall when there is more large-scale precipitation. BC concentrations near the surface increase up to an order of magnitude from case A1 to A2 in October. The ratios in Figures 1e and 1f are strongly anticorrelated with the BC concentrations in Figures 1a and 1b or Figures 1c and 1d. This suggests that the seasonal cycle of BC is strongly modulated by the seasonal cycle of large-scale precipitation [*Garrett et al.*, 2011].

[10] Figure 2 compares modeled BC surface air concentrations with observations at different polar sites. All four basic cases simulate a reasonable seasonal cycle of BC with C1/C2 performing slightly better at Alert, Canada and the South Pole. At the two sites in the Northern Hemisphere (NH) (Barrow, Alaska and Alert, Canada), BC concentrations simulated by C1 and A1 are about 1 to 2 orders of smaller than observed values, especially in early spring. With reduced wet deposition of BC, the modeled BC concentration increases by a factor of ∼4 from C1 to C2 and a factor of ∼6 from A1 to A2. However, C2 and A2 still under-predict the BC concentrations, except in some summer months. At the two Southern Hemisphere (SH) sites (South Pole and Halley, Antarctica), C1/A1 also under-predict the BC concentrations, but they are within one order of magnitude of the observations. With the reduced wet deposition treatment, BC concentrations from C2 and A2 match the observed BC much better. The reason why the models perform better in the SH is due to the relative importance of wet and dry deposition of BC in the two hemispheres. For example, in case C1 wet deposition (mainly by large-scale precipitation) accounts for ∼86% of the total BC deposition at the two NH sites whereas it is only about ∼71% at the two SH sites due to smaller large-scale precipitation in Antarctica. The fact that C2/A2 still under-predict the BC concentrations in the NH suggests that the lifetime of BC, especially in cold seasons, is still too short even with the reduced wet deposition

[1]Auxiliary materials are available in the HTML. doi:10.1029/2012GL053388.

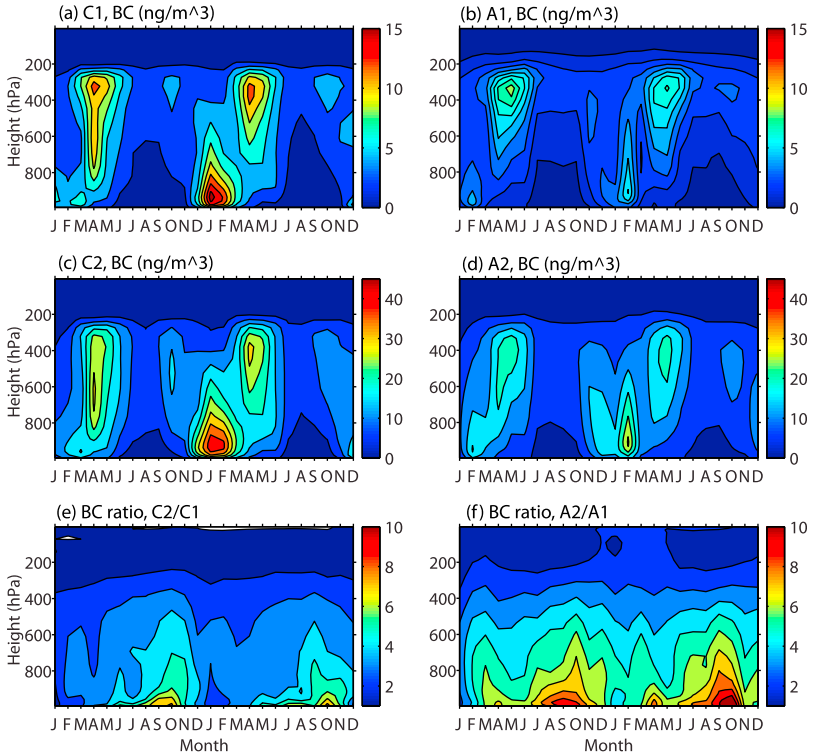

Figure 1. (a–d) Height-time plot of monthly averaged BC concentrations (ng m^{-3}) to the north of 80°N from cases C1, A1, C2 and A2. (e) Height-time plot of ratio of mean BC concentration to the north of 80°N from case C2 to that from case C1. (f) Same as Figure 1e except for cases A2 and A1.

treatment. The wet scavenging efficiency in our model differs between ice and liquid clouds, with the scavenging efficiency set to 10% in ice clouds. If this efficiency is too high, the scavenging could be too large. Moreover, in mixed phase clouds the efficiency is weighted by the fraction of ice and liquid cloud. In addition, the fraction of ice in mixed phase clouds is assumed to be a continuous function of temperature from −40°C to −10°C (Figure S1 in Text S1). If the assumed fraction in the base simulation is too small, the scavenging could be too large. In the sensitivity test case, $C2_{less}$, we used observations of ice nucleation properties for BC and the ice fraction in mixed phase clouds to set the scavenging efficiency and the ice fraction in mixed phase clouds. Thus, the scavenging efficiency of BC was set to be 0.1% for hydrophobic/hydrophilic soot and 3% for hygroscopic soot based on *Koehler et al.* [2009]. The ice fraction was approximately fitted to observations from *Korolev et al.* [2003] (see auxiliary material). As a result, the BC surface concentrations increase by ∼50% but are still generally underestimated especially at the two NH sites (see green line in Figure 2).

[11] Figures 3a–3d show the annual average modeled BC deposition versus the 10-year averaged BC deposition from the ice cores (see Table S1 in Text S1). With larger wet deposition, C1 and A1 under-predict BC concentrations (Figure 2), but the amount of BC deposited on ice matches the observed values more closely, with majority of data points residing within the 2:1 and 1:2 lines. With reduced wet scavenging (cases C2 and A2), the modeled BC deposition at the three sites in Greenland (the three open circles at the upper right corner) improves, but the amount deposited at McBales (the left most open circle) and all SH sites is over-predicted in C2 and A2. With further reduced wet scavenging in ice and mixed phase clouds in case $C2_{less}$, the BC deposition increases by ∼17% over that in case C2 and is overestimated even more than for case C2 at the SH sites.

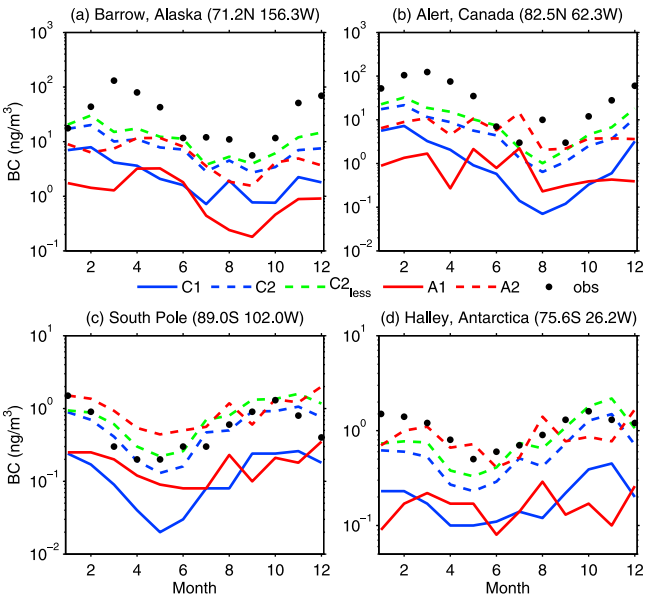

Figure 2. BC concentration at various sites: (a) Barrow, Alaska [*Bodhaine*, 1995], (b) Alert, Canada [*Hopper et al.*, 1994], (c) Amundsen-Scott, South Pole [*Bodhaine*, 1995], (d) Halley, Antarctica [*Wolff and Cachier*, 1998]. Model results are in solid and dashed lines, and observed data are in dots.

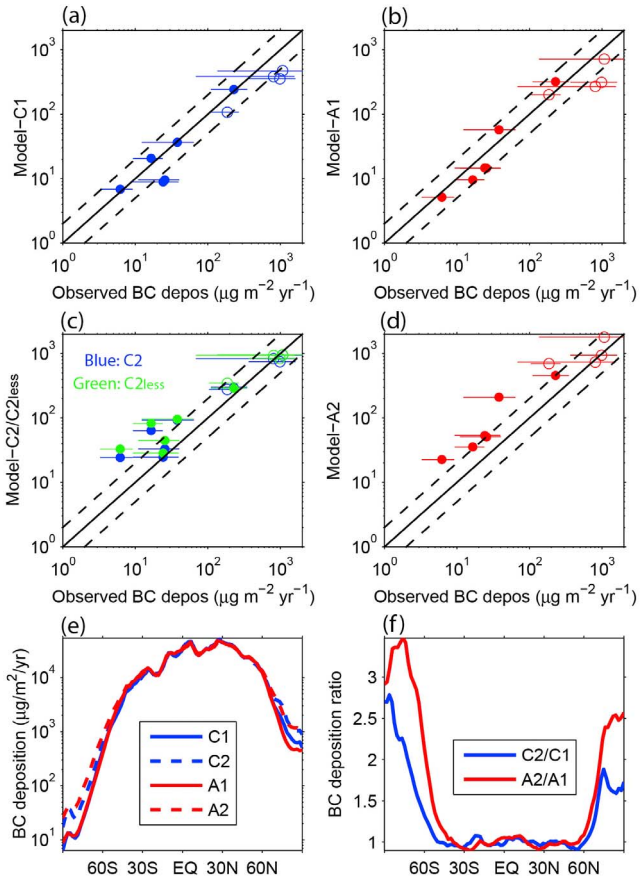

Figure 3. (a–d) Annual average simulated BC deposition (μg m^{-2} yr^{-1}) from models versus the observed 10-year averaged BC deposition from ice cores listed in Table S1 in Text S1 (closed circles: sites in Antarctica; open circles: sites in Greenland). Error bars indicate the standard deviation of the observed BC deposition. The solid lines are 1:1, and the dashed lines are 2:1 or 1:2. (e) Annual zonal mean BC deposition from models. (f) Ratios of annual zonal mean BC deposition from C2 to C1 and A2 to A1.

Figure 3e shows annual zonal mean BC deposition from the baseline models. The amount of BC transported and deposited to the Artic and Antarctica is strongly affected by both differing meteorological fields (compare C1 to A1 and C2 to A2) and wet deposition treatments (compare C1 to C2 and A1 to A2). Figure 3f shows ratios of annual zonal mean BC deposition from C2 to C1 and A2 to A1. The amount of BC deposited in the Arctic increases by a factor of ∼1.7 from C1 to C2 and by a factor of ∼2.5 from A1 to A2. In Antarctica, which is further from the source regions of BC, the increase is even larger: a factor of ∼2.3 from C1 to C2 and a factor of ∼3.3 from A1 to A2.

[12] The global mean radiative forcing (all BC minus no BC) caused by BC deposited to snow and sea-ice is about +0.020 W m^{-2} for both C1 and A1. With reduced wet deposition, the annual mean forcing in the Arctic (>66.5°N) increases from +0.10 to +0.12 W m^{-2} (C1 to C2), and from +0.09 to +0.16 W m^{-2} (A1 to A2). However, the global mean forcing remains unchanged from C1 to C2 and only increases moderately to +0.023 W m^{-2} from A1 to A2, even though the amount of BC deposited in polar regions increases by a factor of ∼2 (Figure 3f). This is because forcing in the Arctic only accounts for ∼20% and ∼30% of the global mean forcing in the IMPACT-CAM5 runs and IMPACT-AM3 runs, respectively. In addition, the BC snow forcing in middle latitudes decreases (see Figure S3 and S4 in Text S1) due to the slight decrease of BC deposition. The global mean BC snow forcing peaks in February while the mean BC snow forcing in the Arctic peaks in April. The mean forcing in the Arctic during spring (March, April and May) is +0.29 W m^{-2} in C1 and +0.27 W m^{-2} in A1, and increases to +0.37 W m^{-2} in C2 and to +0.50 W m^{-2} in A2. Figure 4 shows the Arctic spring BC snow radiative forcings from C2 and A2. The largest forcing occurs in Northern Eurasia and Greenland. Locally, it can be as large as +1 W m^{-2}.

4. Conclusion and Discussion

[13] The transport of black carbon (BC) to polar regions was studied using the University of Michigan IMPACT aerosol model driven by two sets of meteorological fields from the NCAR CAM5 and GFDL AM3 models. BC concentrations and deposition in polar regions are sensitive to both the meteorological fields and the wet deposition

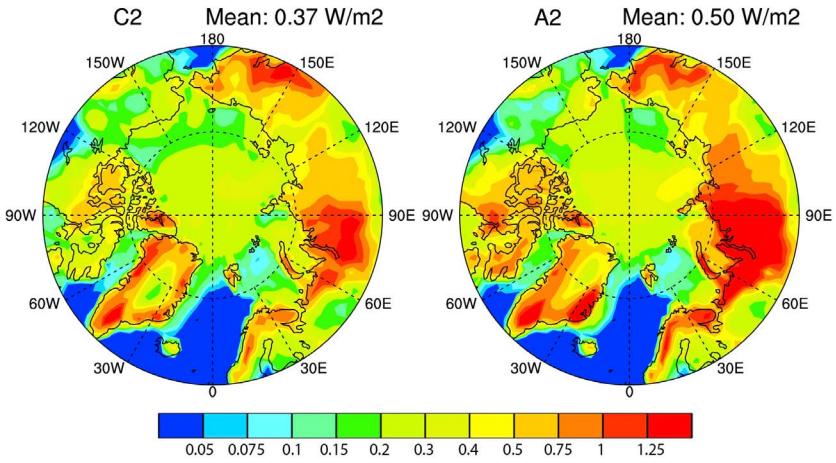

Figure 4. Seasonal mean BC snow radiative forcing in the Arctic in spring (March, April and May) from cases C2 and A2.

treatment. With the baseline treatment for wet deposition, both IMPACT-CAM5 and IMPACT-AM3 models simulate the amount of BC deposition and the seasonal cycle of BC concentrations reasonably well. However, BC surface air concentrations are underestimated. On average, CAM5 meteorological fields transport more BC to the Arctic due to their smaller large-scale precipitation in the NH middle latitudes, smaller in-cloud liquid water content and smaller cloud fractions in NH high latitudes.

[14] With reduced wet deposition in C2 and A2, the near surface BC concentrations increase by a factor of ~3–10 and match observations better, especially in Antarctica; the BC deposition increases by a factor of ~1.7–2.5 in the Arctic and a factor of ~2.3–~3.3 in the Antarctic. IMPACT-AM3 runs are more sensitive to this change because of greater large-scale precipitation in AM3 in the NH middle latitudes. Though simulated near surface BC concentrations improve, they are still underestimated at two NH sites especially in winter and early spring while BC deposition tends to be overestimated in Antarctica. This discrepancy between the simulated BC concentration and deposition may be due to the different observation sites used for BC concentrations and deposition. It may also be due to the fact the BC ground deposition is more related to the whole column concentration rather than the surface concentration. Thus, surface concentrations may be too small if the residence time of BC near the surface is too short or if BC is depleted too quickly above the surface before it can reach to the surface through mixing or gravitational setting. Either result would allow deposition to match observations, while surface concentrations were too small. The discrepancy between surface concentrations and deposition was eased to some extent but not resolved in the sensitivity test case $C2_{less}$ which reduced the rate of wet deposition in ice and mixed phase clouds. *Browse et al.* [2012] also noted the importance of wet deposition in ice clouds, which improved the seasonal concentration cycle in his model. However, they did not have access to the deposition data shown here, and hence were unaware of the lack of congruence between BC surface concentrations and deposition. Further research is needed to resolve this issue.

[15] The mean radiative BC snow forcing in polar regions is also sensitive to the wet deposition treatment and differing meteorological fields. With varying large-scale deposition treatments, the annual mean forcing in the Arctic ranges from +0.10 W m^{-2} to +0.12 W m^{-2} for IMPACT-CAM5 and from +0.09 W m^{-2} to +0.16 W m^{-2} for IMPACT-AM3; in the spring season, the Arctic forcing increases from +0.29 W m^{-2} to +0.37 W m^{-2} for IMPACT-CAM5 and from +0.27 W m^{-2} to +0.50 W m^{-2} for IMPACT-AM3. However, the global mean forcing is less sensitive to both factors due to the tradeoff between the different contributions to forcing from polar regions and middle latitudes. The global annual mean BC snow forcing is about +0.020 W m^{-2} in IMPACT-CAM5 and +0.022 W m^{-2} in IMPACT-AM3. These values are smaller than those modeled by *Flanner et al.* [2007, 2009], who applied an earlier, coupled land-atmosphere–ocean version of CAM. A key reason for this difference is that the offline configuration of CLM applied here produces less snow cover (and hence less area over which the forcing can operate) in the Tibetan Plateau and northern Asia than when it is coupled with CAM.

[16] **Acknowledgments.** This work was funded by NSF projects AGS-0946739 and ARC-1023387. The collection, chemical measurements, and interpretation of the ice cores were funded by a number of projects including NSF 0538416, 0839093, 0909541, and 1023672, and NASA grant NAG04GI66G. We gratefully acknowledge the assistance of field, logistics, drilling, and laboratory personnel in all these projects. Computer time was provided by the NCAR CISL facility.

[17] The Editor thanks two anonymous reviewers for their assistance in evaluating this paper.

References

Balkanski, Y. J., D. J. Jacob, G. M. Gardner, W. C. Graustein, and K. K. Turekian (1993), Transport and residence times of tropospheric aerosols inferred from a global three-dimensional simulation of ^{210}Pb, *J. Geophys. Res.*, *98*(D11), 20,573–20,586, doi:10.1029/93JD02456.

Bauer, S. E., and S. Menon (2012), Aerosol direct, indirect, semidirect, and surface albedo effects from sector contributions based on the IPCC AR5 emissions for preindustrial and present-day conditions, *J. Geophys. Res.*, *117*, D01206, doi:10.1029/2011JD016816.

Bodhaine, B. A. (1995), Aerosol absorption measurements at Barrow, Mauna Loa and the South Pole, *J. Geophys. Res.*, *100*(D5), 8967–8975, doi:10.1029/95JD00513.

Browse, J., K. S. Carslaw, S. R. Arnold, K. Pringle, and O. Boucher (2012), The scavenging processes controlling the seasonal cycle in Arctic sulphate and black carbon aerosol, *Atmos. Chem. Phys.*, *12*, 6775–6798, doi:10.5194/acp-12-6775-2012.

Donner, L. J., et al. (2011), The dynamical core, physical parameterizations, and basic simulation characteristics of the atmospheric component AM3 of the GFDL global coupled model CM3, *J. Clim.*, *24*, 3484–3519, doi:10.1175/2011JCLI3955.1.

Flanner, M. G., C. S. Zender, J. T. Randerson, and P. J. Rasch (2007), Present-day climate forcing and response from black carbon in snow, *J. Geophys. Res.*, *112*, D11202, doi:10.1029/2006JD008003.

Flanner, M. G., C. S. Zender, P. G. Hess, N. M. Mahowald, T. H. Painter, V. Ramanathan, and P. J. Rasch (2009), Springtime warming and reduced snow cover from carbonaceous particles, *Atmos. Chem. Phys.*, *9*, 2481–2497, doi:10.5194/acp-9-2481-2009.

Garrett, T. J., S. Brattström, S. Sharma, D. E. J. Worthy, and P. Novelli (2011), The role of scavenging in the seasonal transport of black carbon and sulfate to the Arctic, *Geophys. Res. Lett.*, *38*, L16805, doi:10.1029/2011GL048221.

Giorgi, F., and W. L. Chameides (1986), Rainout lifetimes of highly soluble aerosols and gases as inferred from simulations with a general circulation model, *J. Geophys. Res.*, *91*(D13), 14,367–14,376, doi:10.1029/JD091iD13p14367.

Hansen, J., and L. Nazarenko (2004), Soot climate forcing via snow and ice albedos, *Proc. Natl. Acad. Sci. U. S. A.*, *101*, 423–428, doi:10.1073/pnas.2237157100.

Hansen, J., et al. (2007), Climate simulations for 1880–2003 with GISS modelE, *Clim. Dyn.*, *29*, 661–696, doi:10.1007/s00382-007-0255-8.

Holland, M., D. A. Bailey, B. P. Briegleb, B. Light, and E. Hunke (2012), Improved sea ice shortwave radiation physics in CCSM4: The impact of melt ponds and aerosols on Arctic sea ice, *J. Clim.*, *25*, 1413–1430, doi:10.1175/JCLI-D-11-00078.1.

Hopper, J. F., D. E. J. Worthy, L. A. Barrie, and N. B. A. Trivett (1994), Atmospheric observations of aerosol black carbon, carbon-dioxide, and methane in the high Arctic, *Atmos. Environ.*, *28*(18), 3047–3054, doi:10.1016/1352-2310(94)90349-2.

Huang, L., S. L. Gong, C. Q. Jia, and D. Lavoué (2010), Importance of deposition processes in simulating the seasonality of the Arctic black carbon aerosol, *J. Geophys. Res.*, *115*, D17207, doi:10.1029/2009JD013478.

Ito, A., and J. E. Penner (2005), Historical emissions of carbonaceous aerosols from biomass and fossil fuel burning for the period 1870–2000, *Global Biogeochem. Cycles*, *19*, GB2028, doi:10.1029/2004GB002374.

Koch, D., S. Menon, A. Del Genio, S. Warren, R. Ruedy, I. Alienov, and G. Schmidt (2009a), Distinguishing aerosol impacts on climate over the past century, *J. Clim.*, *22*, 2659–2677, doi:10.1175/2008JCLI2573.1.

Koch, D., et al. (2009b), Evaluation of black carbon estimations in global aerosol models, *Atmos. Chem. Phys.*, *9*, 9001–9026, doi:10.5194/acp-9-9001-2009.

Koehler, K. A., P. J. DeMott, S. M. Kreidenweis, O. B. Popovicheva, M. D. Petters, C. M. Carrico, E. D. Kireeva, T. D. Khokhlova, and N. K. Shonija (2009), Cloud condensation nuclei and ice nucleation activity of hydrophobic and hydrophilic soot particles, *Phys. Chem. Chem. Phys.*, *11*, 7906–7920, doi:10.1039/b905334b.

Korolev, A., G. A. Isaac, S. G. Cober, J. W. Strapp, and J. Hallett (2003), Microphysical characterization of mixed-phase clouds, *Q. J. R. Meteorol. Soc.*, *129*, 39–65, doi:10.1256/qj.01.204.

Lawrence, D., et al. (2011), Parameterization improvements and functional and structural advances in version 4 of the Community Land Model, *J. Adv. Model. Earth Syst.*, *3*, M03001, doi:10.1029/2011MS000045.

Liu, H., D. J. Jacob, I. Bey, and R. M. Yantosca (2001), Constraints from ^{210}Pb and ^{7}Be on wet deposition and transport in a global three-dimensional chemical tracer model driven by assimilated meteorological fields, *J. Geophys. Res.*, *106*(D11), 12,109–12,128, doi:10.1029/2000JD900839.

Liu, X. H., J. E. Penner, and M. Herzog (2005), Global modeling of aerosol dynamics: Model description, evaluation, and interactions between sulfate and nonsulfate aerosols, *J. Geophys. Res.*, *110*, D18206, doi:10.1029/2004JD005674.

Liu, J., S. Fan, L. W. Horowitz, and H. Levy II (2011), Evaluation of factors controlling long-range transport of black carbon to the Arctic, *J. Geophys. Res.*, *116*, D04307, doi:10.1029/2010JD015145.

Liu, X., et al. (2012), Toward a minimal representation of aerosols in climate models: Description and evaluation in the Community Atmosphere Model CAM5, *Geosci. Model Dev.*, *5*, 709–739, doi:10.5194/gmd-5-709-2012.

Mari, C., D. J. Jacob, and P. Bechtold (2000), Transport and scavenging of soluble gases in a deep convective cloud, *J. Geophys. Res.*, *105*(D17), 22,255–22,268, doi:10.1029/2000JD900211.

Qian, T., A. Dai, K. E. Trenberth, and K. W. Oleson (2006), Simulation of global land surface conditions from 1948 to 2004. Part I: Forcing data and evaluations, *J. Hydrometeorol.*, *7*, 953–975, doi:10.1175/JHM540.1.

Wang, M., J. E. Penner, and X. Liu (2009), Coupled IMPACT aerosol and NCAR CAM3 model: Evaluation of predicted aerosol number and size distribution, *J. Geophys. Res.*, *114*, D06302, doi:10.1029/2008JD010459.

Warren, S., and W. Wiscombe (1980), A model for the spectral albedo of snow. II: Snow containing atmospheric aerosols, *J. Atmos. Sci.*, *37*, 2734–2745, doi:10.1175/1520-0469(1980)037<2734:AMFTSA>2.0.CO;2.

Wolff, E. W., and H. Cachier (1998), Concentrations and seasonal cycle of black carbon in aerosol at a coastal Antarctic station, *J. Geophys. Res.*, *103*(D9), 11,033–11,041, doi:10.1029/97JD01363.

Zhou, C., J. E. Penner, Y. Ming, and X. L. Huang (2012), Aerosol forcing based on CAM5 and AM3 meteorological fields, *Atmos. Chem. Phys.*, *12*, 9629–9652, doi:10.5194/acp-12-9629-2012.